Linear Processing for Two Way Relay with Uplink SCFDMA and Downlink OFDMA

A Project Report

submitted by

JITHIN R. J.

in partial fulfilment of the requirements
for the award of the degree of

MASTER OF TECHNOLOGY

DEPARTMENT OF ELECTRICAL ENGINEERING
INDIAN INSTITUTE OF TECHNOLOGY MADRAS.

May 2013

THESIS CERTIFICATE

This is to certify that the thesis titled **Linear Processing for Two Way Relay with Uplink SCFDMA and Downlink OFDMA**, submitted by **Jithin R. J.**, to the Indian Institute of Technology, Madras, for the award of the degree of **Master of Technology**, is a bona fide record of the research work done by him under our supervision. The contents of this thesis, in full or in parts, have not been submitted to any other Institute or University for the award of any degree or diploma.

Prof. K Giridhar
Project Guide
Professor
Dept. of Electrical Engineering
IIT-Madras, 600 036

Prof. Arun Pachai Kannu
Project Co-Guide
Assistant Professor
Dept. of Electrical Engineering
IIT-Madras, 600 036

Place: Chennai

Date: 16th MAY 2013

ACKNOWLEDGEMENTS

I would like to convey my inexpressible gratitude to my guides, Dr. K. Giridhar and Dr. Arun Pachai Kannu for their constant support, and invaluable advice throughout the duration of my project. Without doubt, it is the interest they took in my work, that has been a constant source of inspiration for me, and has enabled me to keep my spirits high for the past few months. In addition, I would also like to thank them for their invaluable suggestions, corrections, and above all - the faith they put in me in assigning this challenging work.

I would like to thank my parents for their love and support, without which it would have been impossible for me to carry my work at IIT Madras. Besides, my sincerest thanks to my cousin and his family for making my stay at Chennai a memorable one.

I would also like to thank staff of EE department for providing and maintaining the facilities in my lab without fail. And last but not the least, I would like to thank my colleagues in lab - Amrit, Kamalakar, Sanjay, Anshuman, Jagdeesh, and Avinash for fruitful discussion on a plethora of topics. I would also like to thank my friends Anoop, Arun, and Jayesh for the intense badminton sessions, and Vaishakh, Nikhil, and Sreekanth who reminded me that the time I spent wasting, was not really wasted.

ABSTRACT

KEYWORDS: Orthogonal Frequency Division Multiplexing; Single Carrier Frequency Dvision Multiple Access; Long Term Evolution; Minimum Mean Square Error Filter; Source Precoding; Two-way Relay

Two Way relaying has been proven to be a good strategy for improving the overall throughput of a system, by extending coverage of Base stations in wireless networks. Although more complex than one way relaying, two way relay offers much higher spectral efficiency owing to the data transfer in both the directions. In our work, we consider two-way relaying in scenario similar to LTE-Advanced where uplink uses SCFDMA and downlink uses OFDMA. We consider mainly two antenna configurations - one where terminal nodes have one antenna each and relay node has two antenna, and second where all the nodes have two antenna.

We consider different relaying schemes in our work, based on the number of antenna at the relay and terminal nodes. Also, for some scenarios, we assume no global channel state information is available at the terminal nodes during Multiple Access phase. Our aim is to design novel physical layer strategies at the relay ,as well as terminal nodes in order to optimise certain performance criterea such as Bit Error Rate(BER), etc. The asymmetry of modulation schemes in uplink and downlink makes the problem interesting, as well as challenging. To the best of author's knowledge, hardly any research papers in the available literature addresses this problem.

TABLE OF CONTENTS

LIST OF TABLES

LIST OF FIGURES

ABBREVIATIONS

ADC	Analog to Digital Converter
BC	BroadCast
BER	Bit Error Rate
BS	Base Station
CCDF	Complementary Cumulative Density Function
CN	Complex Normal
CP	Cyclic Prefix
CSI	Channel State Information
DAC	Digital to Analog Converter
DFT	Discrete Fourier Transform
DFDMA	Distributed Frequency Domain Multiple Access
DL	Downlink
FDD	Frequency Division Duplexing
FFT	Fast Fourier Transform
IDFT	Inverse Discrete Fourier Transform
ICI	Inter Carrier Interference
IFDMA	Interleaved Frequency Domain Multiple Access
ISI	Intersymbol Interference
LFDMA	Localized Frequency Domain Multiple Access
LTE	Long Term Evolution
MAC	Multiple Access
MIMO	Multiple In Multiple Out
MMSE	Minimum Mean Square Error
MS	Mobile Station
OFDM	Orthogonal Frequency Division Multiplexing
PAPR	Peak to Average Power Ratio
RN	Relay Node

SC-FDMA	Single-Carrier Frequency Domain Multiple Access
SIC	Successive Interference Cancellation
SNR	Signal to Noise Ratio
TDD	Time Division Duplexing
TWRC	Two Way Relay Channel
UL	Uplink
ZF	Zero Forcing

NOTATION

a	Scalar quantity 'a' denoted by lowercase normal font
$\mathbf{a}$	Vector quantity denoted by lowercase boldface
$\mathbf{A}$	Matrix denoted by uppercase boldface
$(.)^T$	Matrix Transpose operation
$(.)^\dagger$	Matrix Transpose operation
$(.)^H$	Matrix Hermitian operation
$(.)^*$	Matrix Conjugate operation
$tr(.)$	Matrix Trace operation
$\mathbb{E}(.)$	Expectation Operation
$\mathbf{I}_n$	Identity matrix of size $n \times n$
$\mathbf{F}_M$	Fourier Transform Matrix of size $M \times M$
$\mathcal{CN}(\mu, \Sigma)$	Circularly Symmetric Complex AWGN of mean μ and Covariance Σ.

CHAPTER 1

Introduction

Due to the path-loss, base stations provide only limited area of coverage for a cellular wireless system. In addition, there are other factors limiting the throughput, such as shadowing, and multipath fading, etc. But due to the recent spurt in demand of high speed data connections it has become necessary to improve the connectivity of existing users, and also to include more number of users. A practical solution to overcome this problem is to use intermediate nodes called Relay Nodes(RN) which help extend the coverage of Base stations, thus improving signal strength of far away users. A Relay node does not source or sink data, but only processes the received data and re-transmits it, so that the performance of the overall system is enhanced.

Though relaying in one direction helps increase performance, it is desirable in some systems to use the relay for bi-directional communication, where systems employs data transfer in both the directions(uplink and downlink). Due to the inherent broadcast nature of wireless channel, it is impossible to avoid interference among nodes which are in proximity of each other. But the two-way relay makes use of this interference (Popovski and Yomo, 2006), (Popovski and Yomo, 2007) in a constructive way. The simplest scheme is Amplify and Forward, where the RN just amplifies the received signal and re-transmits it in such a way that the transmitted signal meets the Relay power constraint. In the following section, other relaying schemes are briefly discussed.

In our work, we consider only a single relay node, and only one pair of users. Besides, all the nodes operate in half duplex mode. As evident from the name, the two-way relay communication takes place in two time slots. In the first time slot, also called Multiple Access Phase(MAC), the two users simultaneously transmit to the RN. In the second time slot, called the Broadcast Phase(BC), the relay broadcasts its signal to the terminal nodes. We consider scenarios where nodes may have single or multiple antenna. For the multipath channel model, we consider only 2 antenna for RN while

terminal nodes can have single or multiple antenna. For the flat-fading channel model, we assume multiple antenna for all the three nodes.

Notations: Scalar quantities are denoted by lower-case letters, vector quantitiesd by boldface lower-case letters, while Matrices are denoted by boldface upper-case letters. $(.)^T$ denotes transpose operation, while $(.)^\dagger$, $(.)^H$, and $(.)^*$ denote the pseudo-inverse, hermitian, and conjugation operations respectively. $tr(.)$ denotes the trace operation, and $\mathbb{E}(.)$ denotes the expectation operation. $\mathbf{I}_n$ denotes an Identity matrix of size $n \times n$. $\mathcal{CN}(\mu, \Sigma)$ denotes circularly symmetric complex gaussian distribution having mean μ, and covariance matrix Σ.

Flow of thesis:

The thesis is organised as follows.

Chapter 2 discusses some of the basic concepts of Two-Way relay, OFDMA and SC-FDMA. It also introduces the aspects of LTE-Advanced based on the existing standards.

Chapter 3 presents various processing strategies at the Relay in the absence of CSI-T at the terminal nodes for the multipath channel model. We present various simulation results for the schemes presented based on LTE-A scenario with and without error control coding.

Chepter 4 analyses the single path flat-fading channel model in the presence of global CSI at all nodes. Here we present an improved algorithm for Source precoding Rajeshwari and Krishnamurthy (2011) , Wang and Tao (2012) based on iterative precoding design.

Finally chapter 5 gives the conclusion of our work.

CHAPTER 2

Basics and Background

2.1 OFDMA and SCFDMA

2.1.1 OFDM Basics

One of the most fundamental function of any communication scheme is to remove the effect of distortion caused by the channel. This equalization operation becomes complex for channels with multiple paths(in complex baseband equivalent model). Also, the multipath channel corresponds to different gains at different frequencies in the frequency domain. Since future wireless communication are poised to use hugh bandwidths, equalization becomes a challenging task if we go for the conventional equalisers. One solution to overcome this difficulty is to use multiple carriers in the bandwidth assigned ,so that, each carrier sees a narrowband flat fading channel which can be equalized easily. This is the basic idea behind Orthogonal Frequency Division Multiplexing(OFDM).

Let us consider two complex baseband sinusoidal signals for a time period T and having frequencies $\frac{k_1}{T}$ and $\frac{k_2}{T}$.

$$s_1(t) = e^{j2\pi\frac{k_1}{T}t} \quad 0 \leq t \leq T \tag{2.1}$$

$$s_2(t) = e^{j2\pi\frac{k_2}{T}t} \quad 0 \leq t \leq T \tag{2.2}$$

where, k_1 and k_2 are integers. It is easily seen that $s_1(t)$ and $s_2(t)$ are orthogonal.

$$< s_1(t), s_2(t) >= \int_0^T e^{j2\pi\frac{k_1}{T}t} e^{-j2\pi\frac{k_2}{T}t} dt = \int_0^T e^{j2\pi\frac{(k_1-k_2)}{T}t} = 0 \text{ for } k_1 \neq k_2 \tag{2.3}$$

So if we modulate two finite duration sinusoids of appropriate frequency and time period T, we can recover the symbols by correlating with the necessary sinusoid of time

period T. The condition for orthogonality is that frequency should be an integral multiple of $\frac{1}{T}$. Since the sinusoids are of finite duration, their spectrum will be having infinite duration(a sinc pulse) in the frequency domain. Since the frequencies are integral multiples of $\frac{1}{T}$, the sinc pulses will have zero crossings at integral multiples of $\frac{1}{T}$ as shown in the figure below.

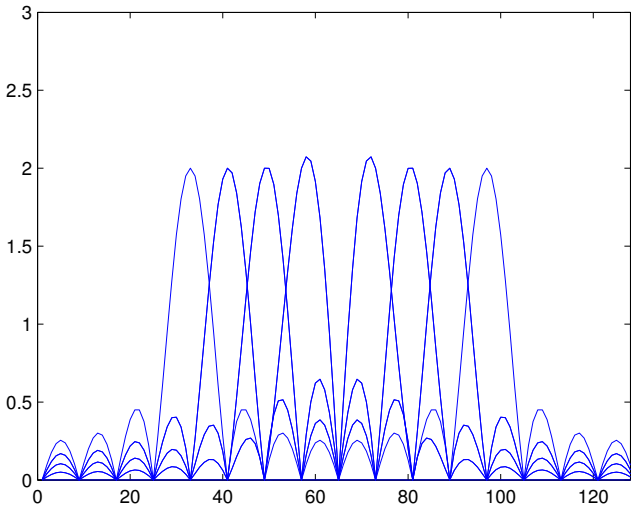

Figure 2.1: The Spectrum of finite duration exponentials used in OFDM

Let N be the number of input symbols for the OFDM transmitter block. This serial stream of symbols, $\mathbf{X}_k$, where $0 \leq k \leq N-1$ is converted to a parallel stream, and the N complex sinusoids are modulated with these N symbols. Therefore, at the $k-th$ subcarrier, the signal is $X_k e^{j2\pi \frac{k}{T} t}$. Since the N complex sinusoids are orthogonal are proved earlier, we can simultaneously transmit these N sinusoids together with the assurance each symbol can recovered completely without interference from adjacent sinusoids. Let the time period be T, and sampling time be $T_s = \frac{T}{N}$.

$$x(t) = \sum_{k=0}^{N-1} X_k e^{j2\pi \frac{k}{T} t} \tag{2.4}$$

The complex baseband equivalent is given as

$$x[n] = x(t)|_{t=nT_s} = \sum_{k=0}^{N-1} X_k e^{j2\pi \frac{k}{NT_s} nT_s} = \sum_{k=0}^{N-1} X_k e^{j2\pi \frac{k}{N} n} \tag{2.5}$$

The last step is the IDFT operation, which can be very efficiently implemented using IFFT algorithm.

When the time domain signal is transmitted through an L-tap multipath channel $h[n]$, whose amplitude is Rayleigh distributed, we expect the linear convolution to occur between $x[n]$ and $h[n]$. But if we convert this linear convolution into circular convolution, then in the frequency domain, the operation becomes a simple multiplication of DFT values of $x[n]$ and $h[n]$ at each subcarrier. That is

$$Y_k = X_k H_k + W_k \tag{2.6}$$

where H_k is the DFT value the $k-th$ subcarrier. $H_k = \sum_{l=0}^{L-1} h[l] e^{j2\pi \frac{k}{N} l}$. The time domain noise samples are circularly symmetric complex AWGN samples $\sim CN(0, N_0)$, and N_0 is the one sided power spectral density.

Inorder to convert the linear convolution into circular convolution, we append the last L of $x[n]$ to the beginning of $x[n]$. This is called Cyclic Prefix. Since the transmitter may not be always aware of L, it prefixes N_{cp} values of the tail of $x[n]$ to the beginning of $x[n]$. Usually N_{cp} is greater than L for the circular convolution to work. Thus, by adding cyclic prefix(CP), the channel matrix in frequency domain reduces to a simple diagonal matrix. Now, the equalization can be performed for each subcarrier independently in a less complex manner since there is only one tap per symbol. We have effectively converted a complex multipath channel into large number of low complexity parallel subchannels. The narrow band subchannels have flat frequency response for which simple equalization techniques can be used.

2.1.2 OFDM Transceiver Model

In the previous section, we explained the basic OFDM model. The subcarriers are overlapping(because of finite duration of time domain signal) but they are orthogonal to each other because each sub-carrier frequency is integral multiple of $\frac{1}{T}$. Thus the subcarriers need not be seperated by guard band inorder to ensure they do not interfere. This gives high spectral efficiency for OFDM transmission.

Below we present the block diagram for OFDM transmission model.

The first block converts a serial stream of symbols to parallem stream. Then the symbols are mapped to their respective subcarriers. After subcarrier mapping the IDFT block converts the frequency domain signals to time domain signals. The cyclic prefix is added, pulse shaping is done and the samples are sent to DAC for passband conversion.

At the receiver, after passband to baseband data conversion, the ADC samples the signal and input to DFT block. The DFT block(implemented using the FFT algorithm) converts the received samples into frequency domain. After equalization for each subcarrier, the decoder decodes the symbols and gives them to turbo decoder for decoding the coded bits.

2.2 Limitations of OFDM

Although OFDM converts a complex multipath channel into narrowband flat fading parallel subchannel, it has some disadvantages with respect to timing and frequency offsets when implemented in real-time.

2.2.1 Timing offset

Timing synchronization is the problem of finding the start of symbol at the receiver. OFDM is highly sensitive to timing because improper timing will result in Intersymbol Interference(ISI), and/or Inter Carrier Interference(ICI). If the timing mismatch is within the CP(but after maximum delay of previous symbol), the demodulation process produces a phase rotation at the output of the FFT which can be corrected using channel estimation. Due to the timing offset of δ smaples, the symbol received at subcarrier k is

$$Y[k] = e^{j2\pi k\delta/N} X[k] \tag{2.7}$$

If the sampling time is within the CP but before the maximum delay of previous symbol, then there will ISI. If the sampling is starting after the CP, then there will be ISI as well as ICI.

2.2.2 Frequency offset

There are two parts to the frequency offset in OFDM. Just like any real number, the frequency offset can be written as $\epsilon = \epsilon_i + \epsilon_f$, where ϵ_i is the integer part, and ϵ_f is the fractional part. ϵ_i is an integer multiple of the subcarrier spacing Δf, and ϵ_f is a fractional part of Δf.

Effect of ϵ_i

In this case ϵ_i will shift cyclically shift symbol mapped in the frequency domain by an amount ϵ_i. So what is received in the $k-th$ subcarrier will be what was sent in $k+\epsilon_i$. The orthogonality of subcarriers will be intact in this case.

$$Y[k] = X[k + \epsilon_i] \tag{2.8}$$

Effect of ϵ_f

In this case, the orthogonality property of the subcarriers is lost because there will be interference from other subcarriers. This will result in amplitude and phase distortion at the $k-th$ subcarrier resulting from the Inter carrier interference.

2.2.3 Peak to Average Power Ratio

The high Peak to Average Power Ratio(PAPR) is a major disadvantge of OFDM. As per the basic principle of OFDM, the time domain sample is the super position of large number of sinusoids of different frequencies with random amplitudes and phase. This causes huge fluctuations in envelope as shown in Fig. 2.2.

The PAPR is defined as the ratio between peak power of a signal to the average power. The average power of the OFDM symbol is given by Frank *et al.* (2008)

$$P_{avg} = \frac{1}{T}\int_{t=0}^{T} |x(t)|^2 dt = \frac{1}{N}\sum_{n=0}^{N-1} |x[n]|^2 \tag{2.9}$$

Therefore, PAPR

$$\zeta = \frac{\max |x[n]|^2}{P_{avg}} \tag{2.10}$$

The PAPR for OFDM is upperbounded by $\zeta \leq N$, where N is the DFT size Slimane (2007).

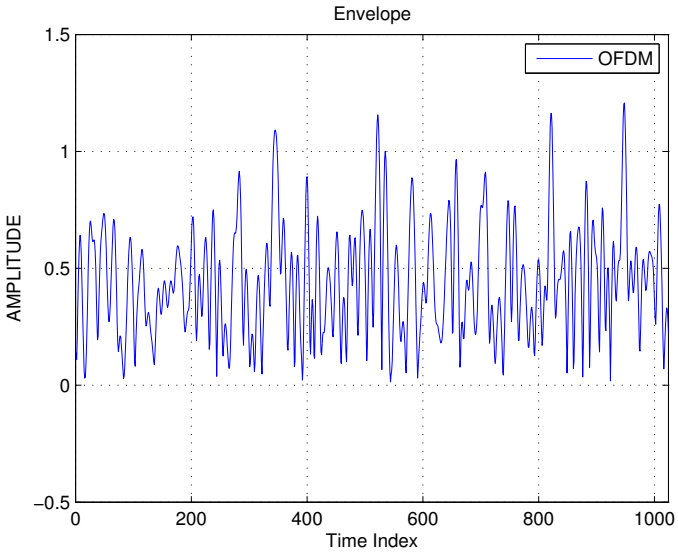

Figure 2.2: Envelope of OFDM for different subcarrier mappings

The large envelope fluctuations causes the power amplifier at the output stage into non linear region. This results in the distortion of OFDM signal, and causes bit error rates to increase. The subcarriers are now no longer orthogonal because of the non linearity. Inorder to decrease the effect of high PAPR, the power amplifier is forced to operate with higher back off from its ideal operating point. This decreases its efficiency causing quicker drainage of battery in mobile devices.

2.2.4 SC-FDMA

In the previous section we saw that the major disadvantage of OFDM was high PAPR. Single Carrier FDMA(SC-FDMA) is a modulation scheme which is a modification of OFDM which has lower PAPR. The basic idea in SC-FDMA is to precode the OFDM symbols before IFFT block. This precoding along with IFFT results in time domain samples which have low PAPR property. The precoding used is DFT precoding, so that

DFT and IDFT cancels out resulting in a single carrier signal in time domain. That's why the name Single Carrier-FDMA.

In practical systems, the number of data streams will be much less than the number of available subcarriers. In that case, the DFT and IDFT will not cancel exactly. The profile of the signal at the output of IDFT block will depend on the subcarrier mapping used in frequency domain Myung *et al.* (2006). There are mainly three types of subcarrier mappings used in SC-FDMA which will heavily influence the PAPR of output signal.

LFDMA

LFDMA stands for Localized Frequency Domain Multiple Access. Here a contiguous block of subcarriers is allocated to a user. Zeros occupy unused subcarriers.

IFDMA

IFDMA stands for Interleaved Frequency Domain Multiple Access. Here the subcarriers are assigned such that they have a uniform number of zero subcarriers between them. Let Q be the number of input symbols after DFT and N be the FFT size of OFDM. $Q \leq N$. If $N = QL$,where L is an integer. In IFDMA, the Q DFT-precoded symbols are mapped every $L - th$ subcarrier, thus occupying entire spectrum.

IFDMA is a special case of DFDMA(Distributed FDMA) where the subcarrier mapping takes place in a distributed manner. Here, the Q subcarriers are divided into groups of $Q_1, Q_2, \ldots, Q_m$ such that $\sum_{k=1}^{m} Q_k = Q$. Each of these groups are mapped such there is no overlapping, and there may or may not be zeros in between them.

The equalization for SC-FDMA modulation is done in frequency domain. After Cyclic prefix removal, the DFT precoded symbols are transformed into frequency domain. This makes the equalization easy becase each subcarrier can be equalized in a simple manner. Then the equalized symbols are transformed back into time domain using $Q - IDFT$ block.

The low PAPR property is illustrated in the figures below. Fig. 2.3 shows the enve-

lope for OFDM, IFDMA, and LFDMA. Without any pulse shaping, IFDMA mapping has the lowest PAPR among all the subcarrier mappings. Fig. 2.4 shows the variation of PAPR with Q. This figure is included because LFDMA is the commonly used mapping scheme in LTE-A rather than IFDMA and DFDMA.

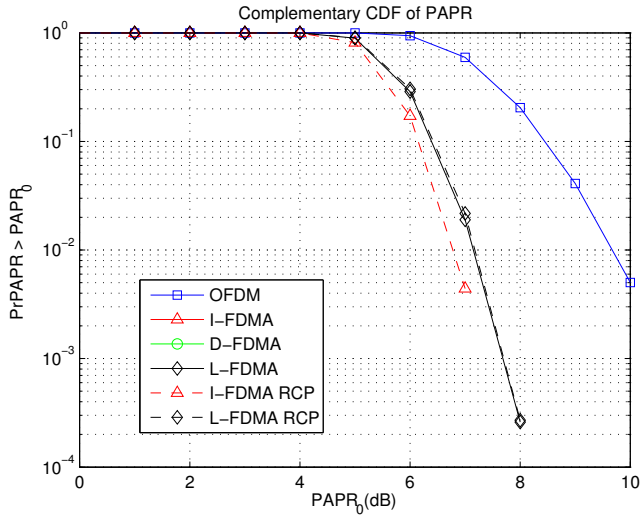

Figure 2.3: CCDF Comparison for different subcarrier mappings

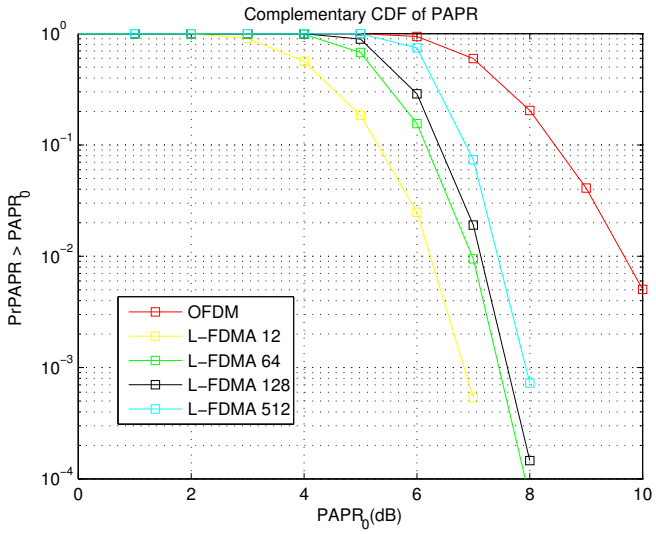

Figure 2.4: CCDF Comparison for LFDMA with varying Q

Because of its low PAPR property, SC-FDMA has been selected as the modulation scheme in user equipment(uplink), while OFDMA will be used in eNodeB(downlink).

2.3 Long Term Evolution

Given the advantages of OFDM communication, LTE uses OFDM Multiplexing technique for downlink and the variant of OFDM, called SC-FDMA for uplink. It supports both Frequency Division Duplexing (FDD) and Time Division Duplexing (TDD) techniques, where the uplink and downlink communication are duplexed in different frequency bands in the former and at different time interval but same frequency bands in the later cases.

2.3.1 Framing Structure

Wide range of bandwidths like 5 MHz, 10 MHz and 20 MHz are supported in LTE 3GPP (2011). The sub-carrier spacing Δf in all these cases is 15 KHz irrespective of the Duplexing mode and Bandwidth and corresponding value for T_u is 66.67 musec. For 10 MHz band-width the sampling rate of the system defined by the standards is 15.36 MHz. OFDM modulation is done using 1024 point IFFT for this system. Out of the 1024 sub-carriers available, the OFDM signal occupies around 667 sub-carriers.

Figure (2.5) and (2.6) shows the time domain structure of the LTE transmission scheme for downlink. Highest level of detail in time is a (Radio) Frame. LTE signal consists of a train of Frames one after the other. A Frame is of length 10ms, which is further divided into 10 subframes each 1ms long. One subframe consists of two 0.5ms long slots. One slot can have either six or seven OFDM symbols. OFDM symbol is the lowest level of detail in time.

It is important to note that LTE downlink scheduling is done on the subframe basis. Stating it otherwise, the LTE downlink Scheduler can change the schedule every subframe.

2.3.2 Extended and Normal CP modes

As it was mentioned in Section (2.3), choice of CP is very important to make sure that IBI and ISI are avoided. Factors that influence the choice of CP are

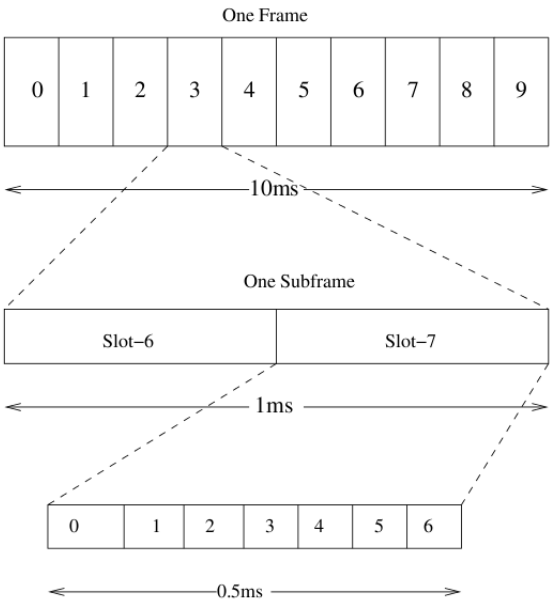

Figure 2.5: Time Domain Structure of an FDD-LTE signal in Normal CP mode 3GPP (2011).

- Maximum delay spread of the channel
- Loss of power due to CP insertion.

If the maximum delay spread of the system is not less than the N_{CP} then the dispersed signal outside the CP will cause (Inter Block Interference)IBI. N_{CP} should be as large as possible if IBI is considered. Reduction of CP will result in increase in errors and hence a loss in power due to compensation. Increment of CP will obviously result in loss of power by a factor $N_{CP}/(N+N_{CP})$ because of redundant transmission. There has to be trade off between both the losses.

Normal cyclic prefix mode: In this mode each slot will contain 7 OFDM symbols. In this mode the first symbol of the slot will have cyclic prefix of length approximately $5.2sec$ where as other 6 symbols have approximately $4.7sec$. This mode is used to provide communication for normal cell size where one can expect shorter channel lengths.

Extended cyclic prefix mode: In this mode each slot will contain 6 OFDM symbols. In this mode all the symbols in the slot will have cyclic prefix of length approximately $10.4sec$. This mode is used to provide communication for very cell size in rural area cells where the CP should be sufficiently long.

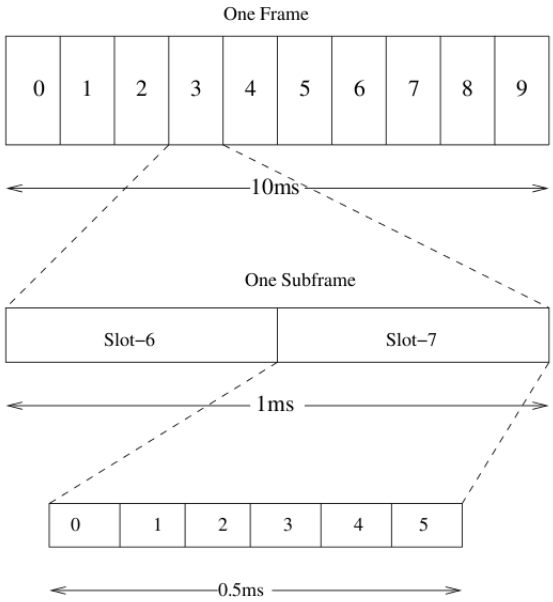

Figure 2.6: Time Domain Structure of an FDD-LTE signal in Extended CP mode 3GPP (2011).

2.4 LTE Frame

An LTE frame is of duration 10 milli seconds which is subdivided into ten 1 millisecond sub-frames. An LTE frame is shown in figure (2.5). An LTE frame is partitioned for uplink and downlink as shown in figure (2.7)

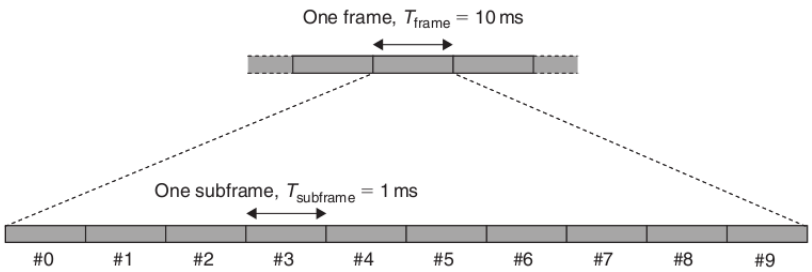

Figure 2.7: LTE frame 3GPP (2011)

In FDD case, bandwidth is shared among uplink and downlink whereas in TDD case, time resources are shared among uplink and downlink. In figure (2.7) it is shown how time domain resources are shared among UL and DL. UL and DL sharing should be dynamic and hence different configurations are specified for TDD UL and DL sharing.

Various configurations for TDD are shown in figure (2.8). One of these configurations is selected by the base station depending on the UL and DL traffic. Of these configurations, some of them are symmetric configurations in which UL and DL resources are shared equally, whereas in the remaining configurations, it is not so.

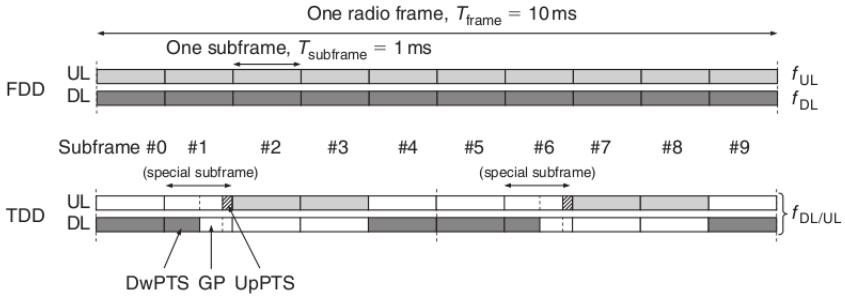

Figure 2.8: LTE UL and DL partitioning in FDD and TDD 3GPP (2011)

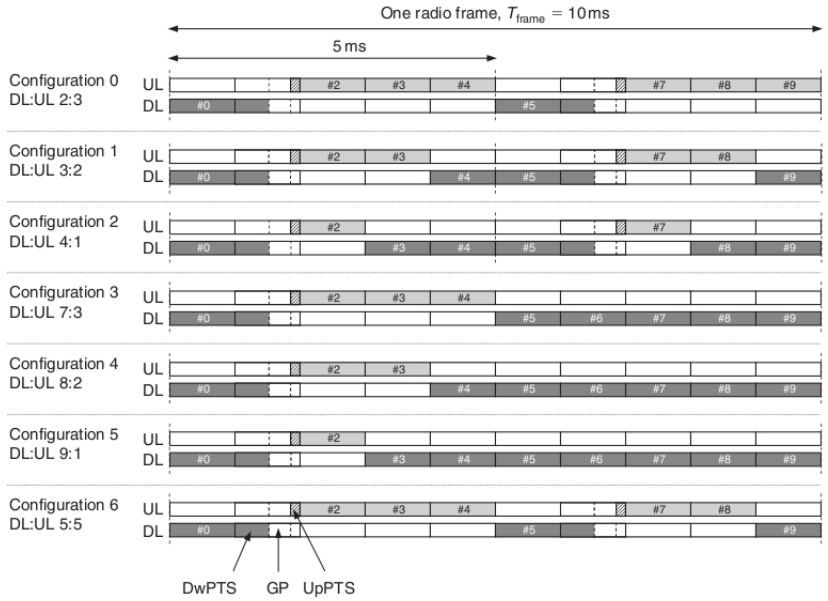

Figure 2.9: Configurations for TDD 3GPP (2011)

The LTE downlink transmission scheme is based on OFDM. OFDM is an attractive downlink transmission scheme for several reasons. Due to the relatively long OFDM symbol time in combination with a cyclic prefix, OFDM provides a high degree of robustness against channel frequency selectivity. Although signal corruption due to a frequency-selective channel can, in principle, be handled by equalization at the receiver

side, the complexity of such equalization starts to become unattractively high for implementation in a mobile terminal at bandwidths exceeding 5 MHz. Therefore, OFDM with its inherent robustness to channel frequency selectivity is attractive for the downlink when extending the bandwidth beyond 5 MHz. Additional benefits with OFDM include:

- OFDM provides access to the frequency domain, and hence enables an additional degree of freedom to the channel-dependent scheduler whereas for HSPA only time-domain scheduling is possible.
- Flexible transmission bandwidth is possible with OFDM, by varying the number of OFDM subcarriers used for transmission.
- Broadcast/multicast transmission, where the same information is transmitted from multiple base stations, is possible with OFDM .
- LTE uplink uses single-carrier transmission based on DFT-spread OFDM (DFTS-OFDM). This single-carrier modulation is used in the uplink because of the lower peak-to-average ratio of the transmitted signal compared to multi-carrier transmission such as OFDM. The smaller the peak-to-average ratio of the transmitted signal, the higher will be the average transmission power for a given power amplifier.

CHAPTER 3

Two Way Relaying and LTE

In this chapter we will characterise the behaviour of two-way relay based on scenario similar to LTE-Advanced. We have done extensive simulation for coded message stream and presented the results for various two antenna configurations. Also, we consider scenario where MS to Relay have lesser SNR than BS to Relay link. This unbalanced SNR is possible in a practical system if the mobile station cannot afford to dissipate as much power as Base station.

When there is no direct link between BS and MS, a relay node acts as an intermediate node to help MS and BS communicate to each other. Conventionally, a relay node supports only unidicrectional communication. But recent advancements have made it possible to develop half duplex [1] relay nodes which support bi-directional communication. The two-way relaying can be classified into several categories depending on the functionality of the relay. 1) Amplify-and-Forward in the which the relay does not decode any signals sent by the source nodes, but precodes the signal before transmission in BC phase so that relay power constraint is met. 2) Decode and Forward relay, in which relay decodes the messages sent by the source nodes, does network coding on them, and broadcasts it in the BC phase, 3) Compress and Forward - in which the relay quantizes the signal received in MAC phase, and broadcasts it in the BC phase. AF Two-way relaying completes its operation in two time slots. The first time slot called Multiple Access(MAC) phase in which both MS and BS transmit to the relay. In the second time slot, called Broadcast(BC) phase, the relay broadcasts its signal to MS and BS. Compared to unidirectional relay, two-way relay is a spectrally efficient protocol because it completes in transmission in two time slots.

Except AF Two-way relay, other protocols need more than two time slots. So AF Two-way relay is an attractive protocol from spectral efficieny point of view. But a major disadvantage with AF relaying is the amplification of noise. The noise in the

[1] We consider only Half Duplex relays in our work.

MAC phase is amplified by the relay and broadcast to terminal nodes. This causes higher bit error rates when compared to other relaying protocols. The use of relay in LTE-A is not yet standardized, and in addition, the use of two way relay for SC-FDMA is uplink/ OFDM in downlink is still an open problem. In this chapter we will evaluate the performance of such a setup in an LTE-Avanced scenario through simulations and analysis.

Fig. 3.1 below shows the block diagram of a two way relay. The MS has N_1 antennas , BS has N_2 antennas while relay has M antennas. The mobile station, hereafter referred to as Node 1, uses SC-FDMA modulation, and BS, hereafter referred to as Node 2, uses OFDM modulation.

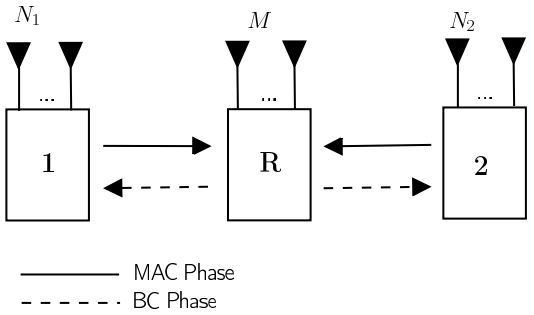

Figure 3.1: Two Way Relay Block diagram

3.1 Channel Model

For our simulations, we consider the multipath channel between the link $1 \leftrightarrow R$ and $2 \leftrightarrow R$. We use the pedestrian B channel model ETSI (2010) in Table 3.1 The channel is assumed to be reciprocal in BC phase.

Power(dB)	0	-0.9	-4.9	-8.0	-7.8	-23.9
Delay(ns)	0	200	800	1200	2300	3700

Table 3.1: Parameters for Pedestrian B Channel model

3.2 Configuration $\mathbf{N}_1 = 1, \mathbf{M} = 2, \mathbf{N}_2 = 1$

We first consider the case when $N_1 = N_2 = 1$ and $M = 2$, and No CSI at terminal nodes, but Relay has global CSI. Let α be the difference in the SNR between Links $1 \rightarrow R$ and $2 \rightarrow R$. Precisely , the SNR difference in dB is $= -10\log(\alpha^2)$ = $SNR_{1\rightarrow R} - SNR_{2\rightarrow R}$. In this case, the terminal nodes can send only one data stream per subcarrier while the relay can decode it, since it has two antennas. For the k-th sub-carrier, the received signal at R during MAC phase is given as

$$\mathbf{y}_r = \mathbf{h}_1 \alpha \sqrt{P_1} x_1 + \mathbf{h}_2 \sqrt{P_2} x_2 + \mathbf{n}_r \tag{3.1}$$

where $\mathbf{y}_r \in \mathbb{C}^{2\times 1}$ is the received signal at R, $\mathbf{h}_1$ is the channel gain of link $1 \rightarrow R$, whose entries are i.i.d. $\mathcal{CN}(0,1)$, x_1 is the DFT-precoded symbol transmitted by node 1, $\mathbf{h}_2$ is the channel gain of link $2 \rightarrow R$, whose entries are i.i.d. $\mathcal{CN}(0,1)$, x_2 is the symbol transmitted by node 2. $\mathbf{n}_r \in \mathbb{C}^{2\times 1}$ is the noise vector whose entries are samples of i.i.d. circularly symmetric complex AWGN. The received signal can be re-written as

$$\mathbf{y}_r = [\mathbf{h}_2\ \mathbf{h}_2] \begin{bmatrix} x_1 \\ x_2 \end{bmatrix} + \mathbf{n}_r \tag{3.2}$$

The MMSE filter for estimating x_1 and x_2 is

$$\mathbf{W}_{mmse} = \left(\mathbf{H}\mathbf{R}_{\mathbf{xx}}\mathbf{H}^H + N_0\mathbf{I}\right)^{-1} \mathbf{H}\mathbf{R}_{\mathbf{xx}} \tag{3.3}$$

, where $\mathbf{H} = [\mathbf{h}_1\ \mathbf{h}_2]$, $\mathbf{x} = \begin{bmatrix} x_1 \\ x_2 \end{bmatrix}$ and $\mathbf{R}_{\mathbf{xx}} = \begin{bmatrix} \alpha^2 P_1 & 0 \\ 0 & P_2 \end{bmatrix}$. The estimates of the transmitted obtained are $\begin{bmatrix} \tilde{x}_1 \\ \tilde{x}_2 \end{bmatrix} = \mathbf{W}_{mmse}^H \mathbf{y}_r$. This the end of MAC phase.

For the BC phase, the relay transmits the MMSE estimates of the symbols. The channel is assumed to be reciprocal. The relay maps the symbol to be received at Node 1 onto Antenna 1, and symbols to be received at Node 2 onto Antenna 2. The performance is independent of mapping since interchanging the mapping onto antenna will only result in the exchange of rows of channel matrix. $\mathbf{x}_r = [\tilde{x}_2\ \tilde{x}_1]^T$ are the symbols to be transmitted. This is similar to a 2×2 MIMO scheme with independent data of two

users. The relay does MMSE precoding on $\mathbf{x}_r$. The advantage with precoding is that, the nodes 1 and 2 need not have have any CSI.

The MMSE precoding Soni *et al.* (2009); Joham *et al.* (2005) filter is given by

$$\mathbf{P}_{mmse} = \frac{1}{\gamma}\left((\mathbf{H}^T)(\mathbf{H}^T)^H + N_0\mathbf{I}\right)^{-1}\mathbf{H}^T \tag{3.4}$$

where $\mathbf{H}^T$ is $[\mathbf{h}_1\ \mathbf{h}_2]^T$, and $\gamma = \sqrt{\frac{tr\{(\mathbf{H}^T\mathbf{H}^* + N_0\mathbf{I})^{-2}\mathbf{H}^T\mathbf{H}^*\}}{P_r/2}}$. The factor γ ensures that the power constraint at relay is met.

The signal received at end nodes 1 and 2, after CP removal and DFT operation are (for the $k-th$ subcarrier) is,

$$\begin{bmatrix} y_2 \\ y_1 \end{bmatrix} = \begin{bmatrix} \mathbf{h}_2^T \\ \mathbf{h}_1^T \end{bmatrix} (\mathbf{P}_{mmse})^H (\mathbf{W}_{mmse})^H \mathbf{y}_r + \begin{bmatrix} n_2 \\ n_1 \end{bmatrix} \tag{3.5}$$

$$= \begin{bmatrix} \mathbf{h}_2^T \\ \mathbf{h}_1^T \end{bmatrix} (\mathbf{P}_{mmse})^H (\mathbf{W}_{mmse})^H [\mathbf{h}_1\ \mathbf{h}_2] \begin{bmatrix} x_1 \\ x_2 \end{bmatrix} + \begin{bmatrix} \mathbf{h}_2^T \\ \mathbf{h}_1^T \end{bmatrix} (\mathbf{P}_{mmse})^H (\mathbf{W}_{mmse})^H \mathbf{n}_r + \begin{bmatrix} n_2 \\ n_1 \end{bmatrix} \tag{3.6}$$

3.2.1 MMSE-SIC Decoding at Relay

Since there are only two streams to be decoded, a Successive Interference Cancellation with multiple iterations for decoding the symbols is also implemented. Note that this is applicable only during MAC phase. The BC phase remains same as mentioned above, with no change in the precoding strategy. For a given iteration, symbols of node 2 are estimated first, then it's interference is removed from the received signal. Then node 1's symbols are decoded. MMSE decoding is implemented for obtaining estimates of the symbols.

$$\mathbf{W}_{2,mmse} = \left(\mathbf{H}\mathbf{R}_{\mathbf{xx}}\mathbf{H}^H + N_0\mathbf{I}\right)^{-1}\mathbf{h}_2\sqrt{P_2} \tag{3.7}$$

$$\tilde{x}_2 = \mathbf{W}_{2,mmse}{}^H\mathbf{y}_r \tag{3.8}$$

with $\mathbf{H}$ and $\mathbf{R}_{\mathbf{xx}}$ defined same as in previous section. After this step, the effect of $\tilde{x}_2$ removed from $\mathbf{y}_r$ to obtain $\tilde{\mathbf{y}}_r$. Following this, the symbols of node 1 are estimated via

MMSE filtering and it's interference is removed from $\tilde{\mathbf{y}}_r$.

$$\tilde{\mathbf{y}}_r = \mathbf{y}_r - \mathbf{h}_2\sqrt{P}_2\tilde{x}_2 \tag{3.9}$$

$$\mathbf{W}_{1,mmse} = \left(\mathbf{h}_1\alpha^2 P_1\mathbf{h}_1^H + N_0\mathbf{I}\right)^{-1}\mathbf{h}_1\alpha\sqrt{P_1} \tag{3.10}$$

$$\tilde{x}_1 = \mathbf{W}_{1,mmse}{}^H\tilde{\mathbf{y}}_r \tag{3.11}$$

$$\tag{3.12}$$

3.2.2 MMSE Processing at Relay and Achievable Rates

In the previous section, we presented SIC algorithm with MMSE detection. Since SC-FDMA symbols are precoded, it will impossible to decode the symbols using ML decoding because of extremely high complexity.Thus sub-optimal alternative method are linear operations such MMSE estimation. The MMSE filtering does not take into account the constellation, and it just minimizes the MSE of transmitted and estimated symbol through linear operation on the received signal. In addition, we have simulated the system with QPSK symbols so that the bias after MMSE processing does not affect the constellation.

Since the relay has as many number of antennas as the number of symbol transmitted, it can estimate the transmitted symbols in the MAC phase. The above mentioned MMSE-SIC algorithm is intractable in terms of analysis, so we resort to a one-shot MMSE estimation of symbols. The MMSE filter for the $k-th$ subcarrier is given by Eqn. 3.3, and the estimates are given by

$$\begin{bmatrix}\tilde{x}_1^{(k)}\\ \tilde{x}_2^{(k)}\end{bmatrix} = \left(\mathbf{W}_{mmse}^{(k)}\right)^H\mathbf{y}_r^{(k)} \tag{3.13}$$

Instead of hard decision denoising at the Relay, let us assume the relay transmits the estimates in the BC phase. Before that, MMSE precoding 3.4 is performed on the estimates.

$$\mathbf{x}_r^{(k)} = \left(\mathbf{P}_{mmse}^{(k)}\right)^H\left(\mathbf{W}_{mmse}^{(k)}\right)^H\mathbf{y}_r^{(k)} \tag{3.14}$$

The received signals at the terminal nodes are(for convinience we drop the super-

script k denoting subcarrier) are explained in Eqn. 3.5.

SINR Analysis

Using equation 3.5 , we will do the SINR analysis of uplink and downlink. The equation can be re-written as

$$\begin{bmatrix} y_2 \\ y_1 \end{bmatrix} = \begin{bmatrix} g_{21} & g_{22} \\ g_{11} & g_{12} \end{bmatrix} \begin{bmatrix} x_1 \\ x_2 \end{bmatrix} + \begin{bmatrix} \tilde{n_2} \\ \tilde{n_1} \end{bmatrix} \tag{3.15}$$

where $g_{ij} = \mathbf{h}_i^T \left(\mathbf{P}_{mmse}\right)^H \left(\mathbf{W}_{mmse}\right)^H \mathbf{h}_j$ and $\tilde{n}_i = \mathbf{h}_i^T \left(\mathbf{P}_{mmse}\right)^H \left(\mathbf{W}_{mmse}\right)^H \mathbf{n}_r + n_i$.

The SINR is defined as the ratio of desired signal energy to the avarage energy of interference and noise. For the OFDM received symbol at node 1, y_1, the desired signal energy is

$$P_b = |g_{12}|^2 \tag{3.16}$$

and the unwanted interference plus noise energy is

$$P_n = |g_{11}|^2 + N_0 \left(\mathbf{h}_1^T \left(\mathbf{P}_{mmse}\right)^H \left(\mathbf{W}_{mmse}\right)^H \mathbf{W}_{mmse}\mathbf{P}_{mmse}\mathbf{h}_1^* + 1\right) \tag{3.17}$$

The SINR is thus $\frac{P_b}{P_n}$ and the end-to-end ergodic rate for downlink($2 \rightarrow 1$) is given

$$R_{21} = \mathbb{E}_{\mathbf{H}} \left[\log_2 \left(1 + \frac{P_b}{P_n}\right)\right] \tag{3.18}$$

For SINR analysis of Uplink, we follow the analysis done in Lin *et al.* (2010). Let $\mathbf{s}_1$ be the time domain symbols of node 1. They are transformed into frequency domain to obtain $\mathbf{x}_1$

The $k-th$ received symbol is

$$\tilde{s}_1^k = \mathbf{F}_M^H(k,:)\mathbf{B}\mathbf{F}_M\mathbf{s}_1 + \mathbf{F}_M^H(k,:)\mathbf{A}\mathbf{x}_2 + \mathbf{F}_M^H(k,:)\tilde{\mathbf{n}} \tag{3.19}$$

where $\mathbf{B} = \text{diag}(g_{21}^k)$ and $\mathbf{A} = \text{diag}(g_{22}^k)$. $\mathbf{F}_M^H(k,:)$ denotes the $k-th$ row of the hermitian of DFT Matrix $\mathbf{F}_M$.

The desired signal energy is

$$P_S = \mathbf{F}_M^H(k,:)\mathbf{B}\mathbf{F}_M(:,k)\mathbf{F}_M^H(k,:)\mathbf{B}^H\mathbf{F}_M(:,k) \tag{3.20}$$

The total received signal energy is

$$P_T = \mathbf{F}_M^H(k,:)\mathbf{B}\mathbf{F}_M\mathbf{F}_M\mathbf{B}^H\mathbf{F}_M(:,k) + \mathbf{F}_M^H(k,:)\mathbf{A}\mathbf{A}^H\mathbf{F}_M(:,k) \tag{3.21}$$

The noise energy is given by

$$P_N = \mathbf{F}_M^H(k,:)\mathbf{C}\mathbf{C}^H\mathbf{F}_M(:,k) \tag{3.22}$$

where

$$\mathbf{C} = \mathbb{E}\left(\tilde{\mathbf{n}}\tilde{\mathbf{n}}^H\right) = \text{diag}\left[N_0\left(\mathbf{h}_1^{T,(k)}\left(\mathbf{P}_{mmse}^{(k)}\right)^H\left(\mathbf{W}_{mmse}^{(k)}\right)^H\mathbf{W}_{mmse}^{(k)}\mathbf{P}_{mmse}^{(k)}\mathbf{h}_1^{*,(k)} + 1\right)\right] \tag{3.23}$$

The SINR is given by $\frac{P_S}{P_T+P_N-P_S}$. The end to end ergodic rate for uplink $(1 \rightarrow 2)$ is given by

$$R_{12} = \mathbb{E}_{\mathbf{H}}\left[\log_2\left(\frac{P_T+P_N}{P_T+P_N-P_S}\right)\right] \tag{3.24}$$

3.3 Configuration $\mathbf{N}_1 = 2, \mathbf{M} = 2, \mathbf{N}_2 = 2$

This configuration, from here on referred to as 2-2-2, is interesting in the sense that Relay cannot decode the symbols sent by nodes 1 and 2 because of less number of antennas than the number of streams which can be sent. In spatial multiplexing mode, we can 2 streams each from 1 and 2 using Amplify and Forward relay processing. In transmit diversity mode, we can send just one stream each from nodes 1 and 2. In next subsection we consider the transmit diversity mode.

3.3.1 Transmit Diversity Mode

We employ Space Frequency coding(SFC) based on the idea of Alamouti for achieving transmit diversity. For terminal $i,\ i \in \{1,2\}$, let $\mathbf{x}_i = \{x_i(0), x_i(1), \ldots, x_i(Q-1)\}$ denote the $1 \times Q$ symbol vector to be transmitted, before sub-carrier mapping. Let two adjacent sub-carriers of antenna $j,\ j \in \{0,1\}$ be denoted as S_j^k and S_j^{k+1}. In the SFC mapping, $x_i(0)$ is mapped to S_0^k, $x_i(Q/2)$ is mapped to S_l^k, $-x_i^*(Q/2)$ is mapped to S_0^{k+1}, and $x_i^*(0)$ is mapped to S_1^{k+1}, and so on. The mapping is summarized below as

$$\longrightarrow \textit{sub-carriers}$$

$$\begin{Bmatrix} x_i(0) & -x_i^*(Q/2) & x_i(1) & -x_i^*(Q/2+1) & \ldots & x_i(Q/2-1) & -x_i^*(Q-1) \\ x_i(Q/2) & x_i^*(0) & x_i(Q/2+1) & x_i^*(1) & \ldots & x_i(Q-1) & x_i^*(Q/2-1) \end{Bmatrix} \tag{3.25}$$

Let channel gains from Tx antenna n to Rx antenna m for node i at sub-carrier k be denoted as $h_{i,m,n}^k$. Then, during MAC phase, the received vector at R at sub-carriers k and $k+1$ are

$$y_0^k = h_{1,0,0}^k x_1(0) + h_{1,0,1}^k x_1(Q/2) + h_{2,0,0}^k x_2(0) + h_{2,0,1}^k x_2(Q/2) + n_{r_0}^k \tag{3.26}$$

$$y_1^k = h_{1,1,0}^k x_1(0) + h_{1,1,1}^k x_1(Q/2) + h_{2,1,0}^k x_2(0) + h_{2,1,1}^k x_b(Q/2) + n_{r_1}^k \tag{3.27}$$

$$y_0^{k+1} = h_{1,0,1}^{(k+1)} x_1^*(0) - h_{1,0,0}^{(k+1)} x_1^*(Q/2) + h_{2,0,1}^{(k+1)} x_b^*(0) - h_{2,0,0}^{(k+1)} x_2^*(Q/2) + n_{r_0}^{k+1} \tag{3.28}$$

$$y_1^{k+1} = h_{1,1,1}^{(k+1)} x_1^*(0) - h_{1,1,0}^{(k+1)} x_1^*(Q/2) + h_{2,1,1}^{(k+1)} x_2^*(0) - h_{2,1,0}^{(k+1)} x_2^*(Q/2) + n_{r_1}^{k+1} \tag{3.29}$$

The above set of equations are re-written as

$$\mathbf{y}_r = \begin{bmatrix} y_0^k \\ y_1^k \\ y_0^{(k+1)*} \\ y_1^{(k+1)*} \end{bmatrix} = \begin{bmatrix} h_{1,0,0}^k & h_{1,0,1}^k & h_{2,0,0}^k & h_{2,0,1}^k \\ h_{1,1,0}^k & h_{1,1,1}^k & h_{2,1,0}^k & h_{2,1,1}^k \\ h_{1,0,1}^{(k+1)*} & -h_{1,0,0}^{(k+1)*} & h_{2,0,1}^{(k+1)*} & -h_{2,0,0}^{(k+1)*} \\ h_{1,1,1}^{(k+1)*} & -h_{1,1,0}^{(k+1)*} & h_{2,1,1}^{(k+1)*} & -h_{2,1,0}^{(k+1)*} \end{bmatrix} \begin{bmatrix} x_1(0) \\ x_1(Q/2) \\ x_2(0) \\ x_2(Q/2) \end{bmatrix} + \begin{bmatrix} n_{r_0}^k \\ n_{r_1}^k \\ n_{r_0}^{(k+1)*} \\ n_{r_1}^{(k+1)*} \end{bmatrix} \tag{3.30}$$

which is of the form $\mathbf{y} = \mathbf{H}\mathbf{x} + \mathbf{n}$. The MMSE estimate of $\mathbf{x}$ can be obtained through the filter given by the same form as 3.3.

During BC phase, we note that the MIMO system is 2×4 system for which there is no zero-forcing or MMSE solution. Also maximum achievable diversity is 2 for a symbol. Therefore, one simple scheme is to map the symbols of nodes 1 and 2 orthogonally onto the subcarriers. For example, if we want node 1 to receive nodes 2's MMSE estimate in BC phase, we transmit nodes 2's MMSE estimates on subcarrier 0. Even though node 2 will also receive these symbols, it will discard them since they are self-interference. The mapping done is shown below. The symbols to be transmitted to node 1 are mapped on to the two transmit antennas of sub-carrier k, while the symbols to be transmitted to node 2 are mapped on the two transmit antennas of sub-carrier $k+1$. This mapping scheme is shown below.

$$\longrightarrow \textit{sub-carriers}$$

$$\begin{Bmatrix} \check{x}_1(0) & \check{x}_2(1) & \check{x}_1(2) & \check{x}_2(3) & \dots & \check{x}_1(Q-1) & \check{x}_2(Q-1) \\ \check{x}_1(1) & \check{x}_2(1) & \check{x}_1(2) & \check{x}_2(3) & \dots & \check{x}_1(Q-1) & \check{x}_2(Q-1) \end{Bmatrix}$$

As in the previous section, precoding is done on each subcarrier as in Eqn. 3.4. Let us examine the operations on node 1's MMSE estimates $[\check{x}_1(0)\ \check{x}_1(1)]^T$. Let $\mathbf{H}_2^T$ be the channel matrix from relay to node 2 in BC phase(assuming reciprocal channel). The precoding matrix is given by

$$\mathbf{P}_{mmse} = \frac{1}{\gamma}\left((\mathbf{H}_2^T)(\mathbf{H}_2^T)^H + N_0\mathbf{I}_2)\right)^{-1}\mathbf{H}_2^T \tag{3.31}$$

where $\gamma = \sqrt{\frac{tr\{(\mathbf{H}_2^T\mathbf{H}_2^* + N_0\mathbf{I})^{-2}\mathbf{H}_2^T\mathbf{H}_2^*\}}{P_r/2}}$.

Following the same analysis as in Eqn. 3.5, we have the estimates of $\check{x}_1(0)$ and $\check{x}_1(1)$ at node 2.

3.3.2 Spatial Multiplexing Mode

As previously discussed, the 2-2-2 configuration can be used in Spatial Multiplexing mode by transmitting two independent data streams from each node. In such a scenario, only Amplify and Forward is possible at the relay since the relay does not have sufficient number of antennas to decode the data streams. Further, in the absence of CSI at the

terminal nodes, it is not feasible to solve the precoding problem at the relay, as the ZF or MMSE solution does not exist. If the terminal nodes have CSI during BC phase, then Relay precoding is possible as done in Lee *et al.* (2008*b*); Zhang *et al.* (2009); Lee *et al.* (2009). They uses optimization based methodology to find the optimum relay precoding matrix, which minimize MSE or maximize sum-rate etc. Neverthless, for comparing the achievable rates of 2-2-2(SM) with 2-2-2(TD), we implement a naive Amplify and Forward scheme with CSI at the terminal nodes only during BC phase.

The signal received at the relay during MAC phase is

$$\begin{bmatrix} y_1 \\ y_2 \end{bmatrix} = \mathbf{H}_1\mathbf{x}_1 + \mathbf{H}_2\mathbf{x}_2 + \mathbf{n}_r \tag{3.32}$$

This received signal is multiplied by the amplification factor γ so that relay power constraint is met.

$$\mathbf{x}_r = \gamma\mathbf{y}_r \tag{3.33}$$

In the BC phase, $\mathbf{x}_r$ is broadcast to both the nodes. Assuming reciprocal channel in BC phase, the signal received at the node i, $i \in (1, 2)$ are

$$\mathbf{y}_i = \mathbf{H}_i^T\mathbf{x}_r + \mathbf{n}_i \tag{3.34}$$

After cancelling self-interference, the received signal at node i is

$$\tilde{\mathbf{y}}_i = \gamma\mathbf{H}_i^T\mathbf{H}_{(3-i)}\mathbf{x}_{(3-i)} + \gamma\mathbf{H}_i^T\mathbf{n}_r + \mathbf{n}_i \tag{3.35}$$

This is equivalent to a MIMO channel with the effective channel matrix given by $\mathbf{H}_{eff,i} = \gamma\mathbf{H}_i^T\mathbf{H}_{(3-i)}$ and noise covariance given by $\mathbf{C}_i = N_0\left(\gamma^2\mathbf{H}_i^T\mathbf{H}_{(3-i)}\mathbf{H}_{(3-i)}^H\mathbf{H}_i^* + \mathbf{I}_2\right)$. Hence, the MMSE filter can be used to decode $\mathbf{x}_{(3-i)}$ at node i.

$$\mathbf{W}_{i,mmse} = \left(\mathbf{H}_{eff,i}\mathbf{H}_{mmse,i}^H + \mathbf{C}_i\right)^{-1}\mathbf{H}_{eff,i} \tag{3.36}$$

$$\tilde{\mathbf{x}}_{(3-i)} = \left(\mathbf{W}_{i,eff}\right)^H\tilde{\mathbf{y}}_i \tag{3.37}$$

The achievable rate Rajeshwari (2012) is

$$R_{i\rightarrow(3-i)} = -\frac{1}{2}\log\det\left(\mathbf{E}_i\right) \tag{3.38}$$

where $\mathbf{E}_i = \mathbb{E}\left[(\mathbf{x}_i - \tilde{\mathbf{x}}_i)(\mathbf{x}_i - \tilde{\mathbf{x}}_i)^H\right]$ is the minimum MSE.

$$\mathbf{E}_i = \left(\mathbf{I} + \mathbf{H}_{eff,i}\mathbf{C}_i^{-1}\mathbf{H}_{eff,i}^H\right) \tag{3.39}$$

3.4 Simulation Results

In this section, we present the simulation results for the two way relay schemes mentioned above. The parameters used for simulation is summarized below.

Paramenter	Value
N(FFT Size)	1024
Q(Used subcarriers)	128
CP Length	64
Modulation	QPSK
Turbo code rate	1/3
Subcarrier Mapping	101 to 228

Table 3.2: Parameters for Simulation

3.4.1 Bit Error Plots

In this subsection, we present the BER plots for the 1-2-1 and 2-2-2(Transmit Diversity mode) schemes explained above. All BER plots are based on Turbo decoding with LTE parameters. Fig. 3.2 shows the BER plot when $\alpha = 0$ dB. That is SNR for uplink and downlink is same for MAC phase.

Fig. 3.3 shows the BER plot for $\alpha = 3dB$.

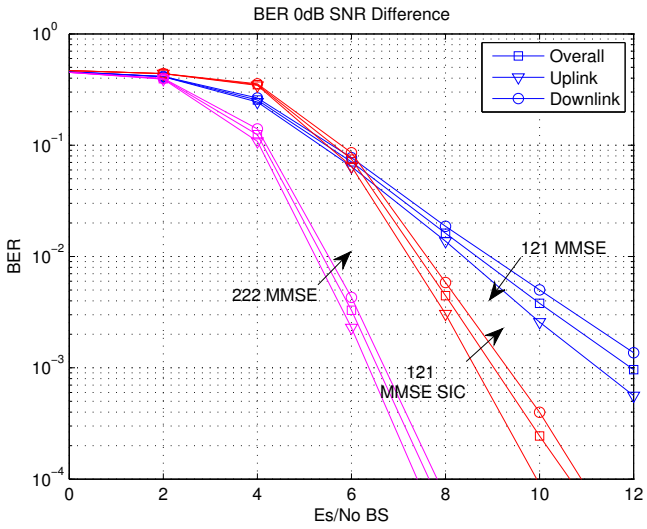

Figure 3.2: BER plot with $\alpha = 0$ dB

3.4.2 Achievable Rates

This subsection illustrates the rate region for the above schemes. The analysis of achievable rates was carried out Section 3.2.2. As shown in the figure, the achievable rate of 222(SM) is the highest since it can transmit two independent streams in both the directions, which is twice that of 1-2-1 scheme. The 222(TD) scheme provides a better rate than 121 but still lesser than 222(SM). At high SNR , as shown in Telatar (1999) , the rate linearly grows as $\min(N_1, M, N_2)$ for both uplink and downlink.

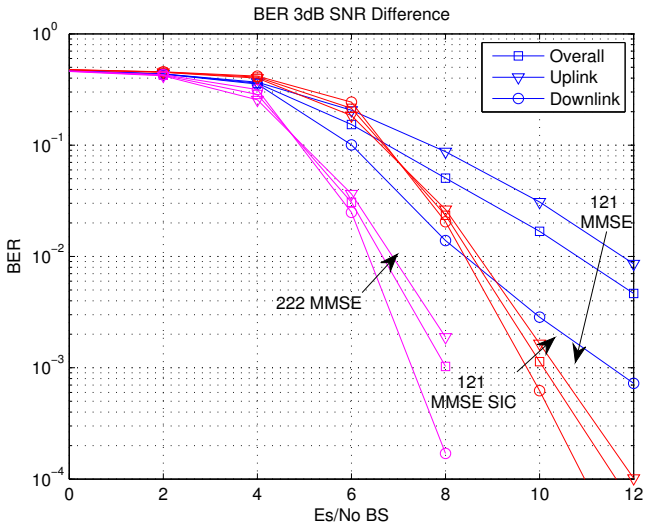

Figure 3.3: BER plot with $\alpha = -3$ dB

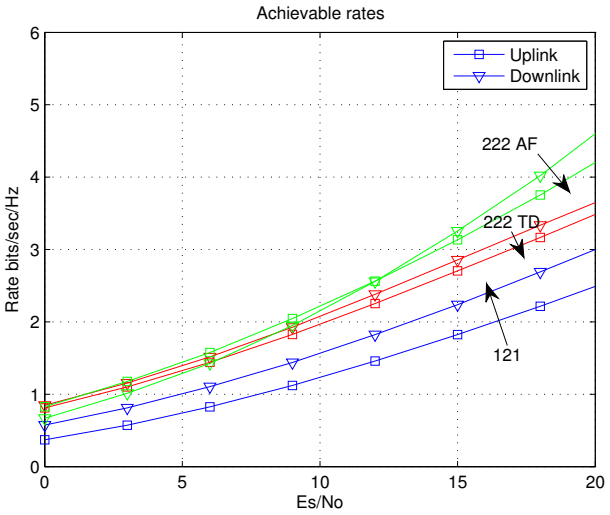

Figure 3.4: Achievable Rates

CHAPTER 4

Two Way Relay with Global CSI

In this chapter we consider the flat fading channel model and assume Global CSI at all the nodes. Since the transmit CSI is available at the terminal nodes, they can do some precoding before transmitting the signals. Minimizing the Mean Square Error(MSE) or maximizing the sum rate has been a widely adopted criteria for the design of Precoders for Two way relay with Global CSI. In Lee *et al.* (2008*a*), authors have shown that nonlinear precoding design, based on constrainted optimization method, performs better than zero-forcing(ZF) and MMSE filtering schemes in terms of BER. By applying gradient descent algorithm, authors in Lee *et al.* (2009) have iteratively designed relay precoders for maximizing sum rate. In Li *et al.* (2010); Havary-Nassab *et al.* (2010); Zhang *et al.* (2009); Shahbazpanahi and Dong (2010), MIMO relay precoder design using constrained optimization was considered but for single antenna at the terminal nodes. For single user, the joint design of source and relay precoders through constrained optimization was considered in Rajeshwari and Krishnamurthy (2011), Wang and Tao (2012) based on MSE critereon. As shown in Rajeshwari and Krishnamurthy (2011) and Wang and Tao (2012), joint iterative design of source and relay precoders gives far more performance benefits than source-only or relay-only precoding.

In AF relaying, one fundamental issue is the noise received in the MAC phase at the relay appearing in the BC phase at the terminal nodes. In our work, we try to address this issue through the widely used wiener filter approach. Instead of applying precoding at the relay, we apply MMSE filter to the received signal at the relay in MAC phase. This effectively mitigates the amount of noise going into the BC phase. This approach not only has low complexity, but also provides better performance when compared to joint source relay precoding, as shown in simulation results. The proposed method is most beneficial when the relay has just enough antennas and processing capabilities to support the given data rate.

The design criterea is to minimize total MSE. Based on this objective, we iteratively

design the source precoder as done in Rajeshwari and Krishnamurthy (2011) and Palomar *et al.* (2003). At each step of iteration, we update the related wiener filter matrices and other constants.

We consider the system shown in Fig. 3.1. Let $\mathbf{H}_1 \in \mathbb{C}^{M\times N_1}$ and $\mathbf{H}_2 \in \mathbb{C}^{M\times N_2}$ be the channel gain matrices from nodes 1 and 2 to the relay respectively. The input signal vector for source i is $\mathbf{x}_i \in \mathbb{C}^{L\times 1}$, and $E(\mathbf{x}_i\mathbf{x}_i^H) = \mathbf{I}_L$. The power constraint at node i is P_i, such that the precoding matrices satisfy the following constraint.

$$\text{tr}(\mathbf{B}_i\mathbf{B}_i^H) \leq P_i, \quad i = 1, 2 \tag{4.1}$$

where $\mathbf{B}_1 \in \mathbb{C}^{N_1\times L}$ and $\mathbf{B}_2 \in \mathbb{C}^{N_2\times L}$ are the precoding matrices at terminal node.

The received complex baseband signal at relay during MAC phase is

$$\mathbf{y}_r = \mathbf{H}_1\mathbf{B}_1\mathbf{x}_1 + \mathbf{H}_2\mathbf{B}_2\mathbf{x}_2 + \mathbf{n}_r \tag{4.2}$$

where $\mathbf{n}_r \in \mathbb{C}^{M\times 1}$ is the realization of random noise vector $\sim CN(0, N_0\mathbf{I}_M)$. Let $\mathbf{G}_r \in \mathbb{C}^{M\times M}$ be the relay processing matrix. We will elaborate on $\mathbf{G}_r$ in the next section as part of proposed algorithm. After the application of relay processing onto the received signal, we get,

$$\mathbf{x}_r = \mathbf{G}_r\mathbf{y}_r \tag{4.3}$$

The resulting signal vector $\mathbf{x}_r$ is transmitted by the relay, and $\mathbf{G}_r$ is designed such that the following relay power contraint is satisfied.

$$\mathbb{E}(\mathbf{x}_r\mathbf{x}_r^H) = \text{tr}\left(\mathbf{G}_r\left[\sum_{i=1}^{2}\mathbf{H}_i\mathbf{B}_i\mathbf{x}_i + N_0\mathbf{I}_M\right]\mathbf{G}_r^H\right) \leq P_r \tag{4.4}$$

In the BC phase, the received signal at node $i,\ (i = 1, 2)$ is

$$\mathbf{y}_i = \mathbf{H}_i^T\mathbf{G}_r\mathbf{H}_i\mathbf{B}_i\mathbf{x}_i + \mathbf{H}_i^T\mathbf{G}_r\mathbf{H}_i\mathbf{B}_{(3-i)}\mathbf{x}_{(3-i)} + \mathbf{H}_i^T\mathbf{G}_r\mathbf{n}_r + \mathbf{n}_i \tag{4.5}$$

After cancelling self interference,

$$\tilde{\mathbf{y}}_i = \mathbf{H}_{eff,(3-i)}\mathbf{x}_{(3-i)} + \tilde{\mathbf{n}}_i \tag{4.6}$$

where $\mathbf{H}_{eff,(3-i)} = \mathbf{H}_i^T \mathbf{G}_r \mathbf{H}_i \mathbf{B}_{(3-i)}$, and $\tilde{\mathbf{n}}_i = \mathbf{H}_i^T \mathbf{G}_r \mathbf{n}_r + \mathbf{n}_i$. The effective noise covariance at node i receiver is therefore $\mathbf{R}_{n,(3-i)} = \mathbb{E}(\tilde{\mathbf{n}}_i \tilde{\mathbf{n}}_i^H) = \mathbf{H}_i^T \mathbf{G}_r \mathbf{G}_r^H \mathbf{H}_i^* + N_0 \mathbf{I}_{N_i}$

The unconstrained optimal receiver filter Rajeshwari and Krishnamurthy (2011), Wang and Tao (2012) is the Wiener filter given by $\mathbf{W}_{(3-i)} = (\mathbf{H}_{eff,(3-i)} \mathbf{H}_{eff,(3-i)}^H + N_0 I)^{-1} \mathbf{H}_{eff,(3-i)}$.

$$\tilde{\mathbf{x}}_{(3-i)} = \mathbf{W}_{(3-i)}^H \tilde{\mathbf{y}}_i \tag{4.7}$$

The minimum mean square error, after filtering for user i, after receiver processing at node $(3-i)$, $(i = 1, 2)$ is given by Palomar *et al.* (2003)

$$\mathbf{E}_i = \mathbb{E}[(\tilde{\mathbf{x}}_i - \mathbf{x}_i)(\tilde{\mathbf{x}}_i - \mathbf{x}_i)^H] = (\mathbf{I} + \mathbf{B}_i \mathbf{R}_{H,i} \mathbf{B}_i^H)^{-1} \tag{4.8}$$

where

$$\mathbf{R}_{H,i} = \mathbf{H}_i^H \mathbf{G}_r^H \mathbf{H}_{(3-i)}^* \mathbf{R}_{N,i} \mathbf{H}_{(3-i)}^T \mathbf{G}_r \mathbf{H}_i \tag{4.9}$$

and

$$\mathbf{R}_{N,i} = \left(\mathbf{I}_{N_{(3-i)}} + \mathbf{H}_{(3-i)}^T \mathbf{G}_r \mathbf{G}_r^H \mathbf{H}_{(3-i)}^* \right)^{-1} \tag{4.10}$$

Our objective now is to minimize the total MSE of both the terminal nodes by designing the source precoding matrices, subject to the power constraints. This problem is formally stated below.

$$\begin{aligned} \min_{\mathbf{B}_1, \mathbf{B}_2} J &= \sum_{i=1}^{2} \text{tr}(\mathbf{E}_i) \\ \text{s. t.} \quad \text{tr}(\mathbf{B}_i \mathbf{B}_i^H) &\leq P_i, \quad i = 1, 2 \end{aligned} \tag{4.11}$$

4.1 Source Precoding and Relay Processing design

In this section we propose the algorithm for minimizing total MSE for the MIMO two way relay system. The design of source precoding matrices was part of the joint source relay precoding design in Rajeshwari and Krishnamurthy (2011), Wang and Tao (2012), Unger and Klein (2008); Lee *et al.* (2010); Xu and Hua (2011) . We deviate from this

approach in that, only source precoding is done iteratively, while relay employs MMSE noise filtering. During each iteration of algorithm, the source precoders are updated as in Rajeshwari and Krishnamurthy (2011), and consequently the relay processing matrix $\mathbf{G}_r$ is updated. The algorithm stops after maximum number of iterations specified is reached or when the objective function converges(whichever is earlier).

4.1.1 Design of Relay processing matrix

We explain the design of the relay processing matrix $\mathbf{G}_r$ for a given set of source precoding matrices. In (2), we let $\mathbf{x}_r = \mathbf{H}_1\mathbf{B}_1\mathbf{x}_1 + \mathbf{H}_2\mathbf{B}_2\mathbf{x}_2$. In order to reduce the amount of noise going into the BC phase from MAC phase, we try to get the MMSE estimate of $\mathbf{x}_r$, which we denote as $\check{\mathbf{x}}_r$. The received relay signal $\mathbf{y}_r$ is

$$\mathbf{y}_r = \mathbf{H}_1\tilde{\mathbf{x}}_1 + \mathbf{H}_2\tilde{\mathbf{x}}_2 + \mathbf{n}_r \tag{4.12}$$

where $\tilde{\mathbf{x}}_i = \mathbf{B}_i\mathbf{x}_i,\ (i = 1, 2)$. Let $\tilde{\mathbf{x}}_r = \mathbf{H}_1\tilde{\mathbf{x}}_1 + \mathbf{H}_2\tilde{\mathbf{x}}_2$. In the next step, try to get the MMSE estimate of $\tilde{\mathbf{x}}_r$.

The Wiener filter for getting the MMSE estimate is $\mathbf{W}_r = (\mathbf{S} + N_0\mathbf{I}_M)^{-1}\mathbf{S}$, where $\mathbf{S} = \mathbb{E}(\tilde{\mathbf{x}_r}\tilde{\mathbf{x}_r}^H) = \mathbf{H}_1\mathbf{B}_1\mathbf{B}_1^H\mathbf{H}_1^H + \mathbf{H}_2\mathbf{B}_2\mathbf{B}_2^H\mathbf{H}_2^H$. Applying wiener filter, we have

$$\hat{\mathbf{y}}_r = \mathbf{W}_r^H\mathbf{y}_r \tag{4.13}$$

$$\check{\mathbf{x}}_r = \alpha\mathbf{W}_r^H\mathbf{y}_r \tag{4.14}$$

Multiplication by α is to ensure that $\check{\mathbf{x}}_r$ meets the relay power contraint (4) after applying MMSE filtering.

$$\alpha = \sqrt{\frac{P_r}{tr\left(\mathbf{W}_r^H\left[\sum_{i=1}^{2}\mathbf{H}_i\mathbf{B}_i\mathbf{x}_i + N_0\mathbf{I}_N\right]\mathbf{W}_r\right)}} \tag{4.15}$$

From (15) it is clear that $\mathbf{G}_r = \alpha\mathbf{W}_r^H$. Thus $\mathbf{G}_r$ ensures mitigation of noise in the BC phase, while meeting the relay power constraint.

4.1.2 Iterative design of source precoders

The iterative design of source precoders follows exact steps as in (Rajeshwari and Krishnamurthy, 2011, Sec.IV.A). For each user, the end to end data transmission is similar to a MIMO system which supports L spatially multiplexed streams. Hence the optimal precoding solution proposed in Palomar *et al.* (2003) holds. Consider the eigen decomposition of $\mathbf{R}_{H,i} = \mathbf{U}_i \mathbf{\Lambda}_i \mathbf{U}_i^H \ (i = 1, 2)$,where $\mathbf{U}_i$ is a unitary matrix containing eigen vectors of $\mathbf{R}_{H,i}$ and $\mathbf{\Lambda}_i$ is the diagonal matrix containing eigen values of $\mathbf{R}_{H,i}$ arranged in the descending order. The optimal precoder will have rank $\tilde{L}_i = min(L, rank(\mathbf{R}_{H,i}))$. The optimal precoder $\mathbf{B}_i$ will be of the form

$$\mathbf{B}_i = \tilde{\mathbf{U}}_i \mathbf{\Sigma}_i \ (i = 1, 2) \tag{4.16}$$

where $\tilde{\mathbf{U}}_i$ consists of first $\tilde{L}_i$ columns of $\mathbf{U}_i$, and $\mathbf{\Sigma}_i = [\text{diag}(\{\sigma_{i,j}\}) \ \mathbf{0}] \in \mathbb{C}^{\tilde{L}_i \times L}, \ \sigma_{i,j} \geq 0, \ (i = 1, 2 \text{ and } j = 1, \ldots, \tilde{L}_i$. The diagonal elements $\sigma_{i,j}$ are given by

$$\sigma_{i,j} = \sqrt{\left(\mu_i^{-1/2} \lambda_{H_{i,j}}^{-1/2} - \lambda_{H_{i,j}}^{-1}\right)^+} \tag{4.17}$$

where $\lambda_{H_{i,j}}$ are the diagonal elements of $\mathbf{R}_{H,i}$, and μ_i is the Lagrangian multiplier chosen to satisfy (1). The iterative algorithm to find the optimal source precoding matrices which minimizes the objective function, $f_{obj} = J$ in (10) is given below.

Algorithm 1. – Iterative Source Precoder design

Initialise $\mathbf{W}_r^{(0)} = (\mathbf{S} + N_0 \mathbf{I}_N)^{-1} \mathbf{S}$, where $\mathbf{S} = \mathbb{E}(\tilde{\mathbf{x}_r} \tilde{\mathbf{x}_r}^H) = \frac{P_1}{L} \mathbf{H}_1 \mathbf{H}_1^H + \frac{P_2}{L} \mathbf{H}_2^H \mathbf{H}_2^H$. Set iteration number $k = 1$ and tolerance ϵ for algorithm termination.

Step 1 Update $\mathbf{B}_i^{(k)} \ i = 1, 2$ using $\alpha^{(k-1)}, \mathbf{W}_r^{(k-1)}$ obtained in the previous step.

Step 2 Substitute for $\mathbf{B}_i^{(k)} \ i = 1, 2$ in $f_{obj}^{(k)}$ and update $\alpha^{(k)}, \mathbf{W}_r^{(k)}$.

Step 3 If $|f_{obj}^{(k)} - f_{obj}^{(k-1)}| \leq \epsilon$, then output $\alpha^{(k)}, \mathbf{W}_r^{(k)}, \mathbf{B}_1^{(k)}, \mathbf{B}_2^{(k)}$. Else go to Step 1.

Output $\mathbf{B}_i$ $i = 1, 2$, α and $\mathbf{W}_r$.

4.2 Simulation Results

In this section we present the simulation results for the proposed algorithm. The $SNR\,(dB)$ is defined as $10\log_{10}\left(\frac{1}{N_0}\right)$, so that a fair comparison is possible with other schemes. All the performance shown have been averaged over 10000 realizations of the channel. It is important to note that we are minimizing the total MSE only with respect to the source nodes. Hence, increasing the number of relay antennas beyond L will not result in substantial performance gains as we will see in the simulation results. But increasing the number of antennas at terminal nodes beyond L will result in significant performance gains. In the latter case ($N_1, N_2 \geq L$), our design gives about 3 to 4 dB improvement for BER at moderate to high SNR as compared to results in Rajeshwari and Krishnamurthy (2011) and Wang and Tao (2012) for $N_1 = N_2 = M = 2$, without the use of any optimization algorithms such as Sequential Quadratic Programming and QCQP. This is evident from Fig. 4.1. If we want to have performance gains with $M \geq L$, we must optimize our objective function w.r.t. relay processing matrix, which is not considered in this work. Since the proposed algorithm does not use any convex optimization package, its complexity will be least compared to the existing joint source relay precoding designs.

Another significant observation we would like to point out is that the proposed algorithm is robust to the power constraints at all nodes, which is shown in Fig. 4.2. We observe no error floor even if power allocated to one terminal node is different than the other. Though not included in simulation results, the proposed algorithm places no restriction on the number of antenna at source nodes. Fig. 4.3 shows behaviour of total MSE and Fig. 4.4 shows the sum-rate achievable under equal power constraints. The sum-rate for proposed algorithm also outperforms the gradient descent algorithm proposed in Lee *et al.* (2009).

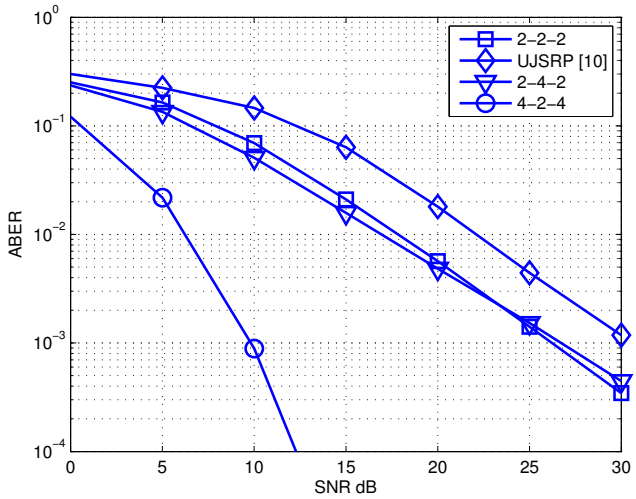

Figure 4.1: Average BER for $P_1 = P_2 = P_r$

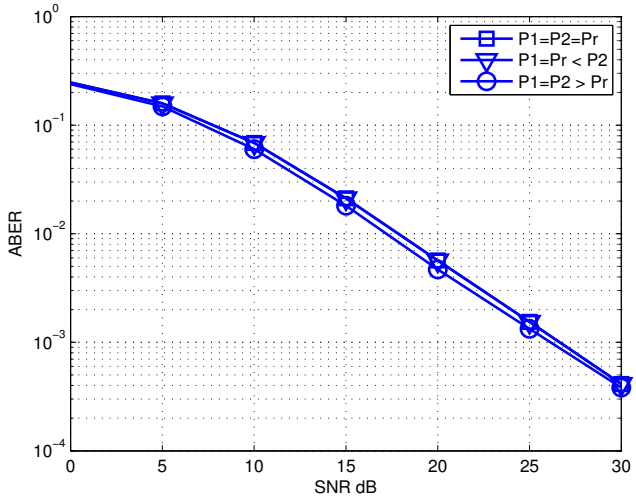

Figure 4.2: Average BER for unequal Power constraints for $N_1 = M = N_2 = 2$

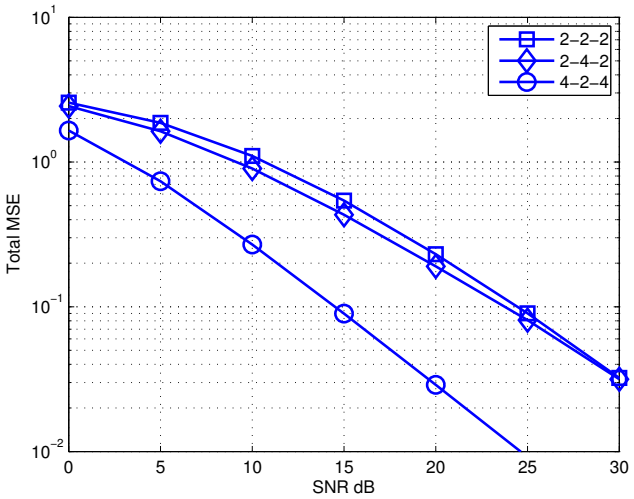

Figure 4.3: Total MSE for $P_1 = P_2 = P_r$

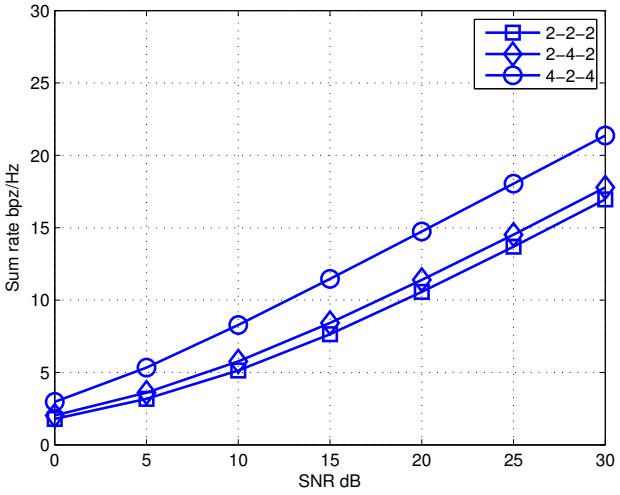

Figure 4.4: Achievable sum-rate for $P_1 = P_2 = P_r$

CHAPTER 5

Conclusion

In this thesis we have evaluated the performance of two-way relay involving uplink SC-FDMA and downlink OFDMA in a LTE-A based set up. For the 1-2-1 and 2-2-2 case, when there is no CSI at the terminal nodese, we have done Linear Processing at the Relay node, which involves getting MMSE estimates of the transmitted symbols by UE and BS. For the BC phase, the relay does preprocessing. The proposed scheme will work for only certain configurations.

For the 2-2-2 case, it is still an open problem in the literature to estimate the transmitted symbols at the relay, when we transmit two independent data streams from each node. Hence we analyse only the achievable rate of such a scheme when AF protocol is used. We observe that AF protocol is spectrally efficient compared 2-2-2(TD) scheme. While observing bit error rates, we have also considered scenarios where uplink has lesser SNR than downlink.

When there is CSI available at all the nodes, it is feasible to do precoding before transmission inorder to improve performance Palomar *et al.* (2003). For such a scenario, we considered the narrow band flat fading rayleigh fading model, and proposed an improved source precoding algorithm. Our algorithm mitigates noise from MAC phase to BC phase. Since we do not do any relay precoding, our algorithm will be advantageous only when there are equal or more number of source antennas than relay antennas.

REFERENCES

1. **3GPP** (2011). 3gpp ts 36.211, "evolved universal terrestrial radio access (e-utra); physical channels and modulation".

2. **ETSI, T.** (2010). 125 996 v. 6.1. 0,"universal mobile telecommunications system (umts); spatial channel model for multiple input multiple output (mimo) simulations (3gpp tr 25.996 version 6.1. 0 release 6)," sept. 2003.

3. **Frank, T.**, **A. Klein**, and **T. Haustein**, A survey on the envelope fluctuations of dft precoded ofdma signals. *In Communications, 2008. ICC'08. IEEE International Conference on*. IEEE, 2008.

4. **Havary-Nassab, V.**, **S. Shahbazpanahi**, and **A. Grami** (2010). Optimal distributed beamforming for two-way relay networks. *Signal Processing, IEEE Transactions on*, **58**(3), 1238–1250.

5. **Joham, M.**, **W. Utschick**, and **J. A. Nossek** (2005). Linear transmit processing in mimo communications systems. *Signal Processing, IEEE Transactions on*, **53**(8), 2700–2712.

6. **Lee, K.-J.**, **K. W. Lee**, **H. Sung**, and **I. Lee**, Sum-rate maximization for two-way mimo amplify-and-forward relaying systems. *In Vehicular Technology Conference, 2009. VTC Spring 2009. IEEE 69th*. IEEE, 2009.

7. **Lee, K.-J.**, **H. Sung**, **E. Park**, and **I. Lee** (2010). Joint optimization for one and two-way mimo af multiple-relay systems. *Wireless Communications, IEEE Transactions on*, **9**(12), 3671–3681.

8. **Lee, N.**, **H. Park**, and **J. Chun**, Linear precoder and decoder design for two-way af mimo relaying system. *In Vehicular Technology Conference, 2008. VTC Spring 2008. IEEE*. IEEE, 2008*a*.

9. **Lee, N.**, **H. J. Yang**, and **J. Chun**, Achievable sum-rate maximizing af relay beamforming scheme in two-way relay channels. *In Communications Workshops, 2008. ICC Workshops' 08. IEEE International Conference on*. IEEE, 2008*b*.

10. **Li, C.**, **L. Yang**, and **W.-P. Zhu** (2010). Two-way mimo relay precoder design with channel state information. *Communications, IEEE Transactions on*, **58**(12), 3358–3363.

11. **Lin, Z.**, **P. Xiao**, **B. Vucetic**, and **M. Sellathurai** (2010). Analysis of receiver algorithms for lte lte sc-fdma based uplink mimo systems. *Wireless Communications, IEEE Transactions on*, **9**(1), 60–65.

12. **Myung, H. G.**, **J. Lim**, and **D. J. Goodman** (2006). Single carrier fdma for uplink wireless transmission. *Vehicular Technology Magazine, IEEE*, **1**(3), 30–38.

13. **Palomar, D. P.**, **J. M. Cioffi**, and **M. A. Lagunas** (2003). Joint tx-rx beamforming design for multicarrier mimo channels: A unified framework for convex optimization. *Signal Processing, IEEE Transactions on*, **51**(9), 2381–2401.

14. **Popovski, P.** and **H. Yomo**, Bi-directional amplification of throughput in a wireless multi-hop network. *In Vehicular Technology Conference, 2006. VTC 2006-Spring. IEEE 63rd*, volume 2. IEEE, 2006.

15. **Popovski, P.** and **H. Yomo**, Physical network coding in two-way wireless relay channels. *In Communications, 2007. ICC'07. IEEE International Conference on*. IEEE, 2007.

16. **Rajeshwari, S.** and **G. Krishnamurthy**, New approach to joint mimo precoding for 2-way af relay systems. *In Communications (NCC), 2011 National Conference on*. IEEE, 2011.

17. **Rajeshwari, S. S.**, Universal approach to linear precoding for two-way amplify and forward mimo relay systems. *In Masters Thesis*. EE Department IIT Madras, 2012.

18. **Shahbazpanahi, S.** and **M. Dong**, Achievable rate region and sum-rate maximization for network beamforming for bi-directional relay networks. *In Acoustics Speech and Signal Processing (ICASSP), 2010 IEEE International Conference on*. IEEE, 2010.

19. **Slimane, S. B.** (2007). Reducing the peak-to-average power ratio of ofdm signals through precoding. *Vehicular Technology, IEEE Transactions on*, **56**(2), 686–695.

20. **Soni, A.**, **T. Sharma**, **M. Chandwani**, and **V. Chakka**, Mimo two-way relaying in frequency selective environment using ofdm. *In Cognitive Wireless Systems (UKIWCWS), 2009 First UK-India International Workshop on*. IEEE, 2009.

21. **Telatar, E.** (1999). Capacity of multi-antenna gaussian channels. *European transactions on telecommunications*, **10**(6), 585–595.

22. **Unger, T.** and **A. Klein**, Maximum sum rate of non-regenerative two-way relaying in systems with different complexities. *In Personal, Indoor and Mobile Radio Communications, 2008. PIMRC 2008. IEEE 19th International Symposium on*. IEEE, 2008.

23. **Wang, R.** and **M. Tao** (2012). Joint source and relay precoding designs for mimo two-way relaying based on mse criterion. *Signal Processing, IEEE Transactions on*, **60**(3), 1352–1365.

24. **Xu, S.** and **Y. Hua** (2011). Optimal design of spatial source-and-relay matrices for a non-regenerative two-way mimo relay system. *Wireless Communications, IEEE Transactions on*, **10**(5), 1645–1655.

25. **Zhang, R.**, **Y.-C. Liang**, **C. C. Chai**, and **S. Cui** (2009). Optimal beamforming for two-way multi-antenna relay channel with analogue network coding. *Selected Areas in Communications, IEEE Journal on*, **27**(5), 699–712.